7-23-2017

Tumor detection and treatment by means of thermography and laser irradiation

Euiheon Chung
Gwangju Institute of Science and Technology, South Korea, ogong50@gist.ac.kr

Gyungseok Oh
School of Mechanical Engineering, GIST

Su Woong Yoo
Department of Nuclear Medicine, Chonnam National University Hwasun Hospital, Korea

TUMOR DETECTION AND TREATMENT BY MEANS OF THERMOGRAPHY AND LASER IRRADIATION

[1,2]Euiheon Chung, [1]Gyungseok Oh, [2]Su Woong Yoo

[1]School of Mechanical Engineering, [2]Department of Biomedical Science and Engineering, Institute of Integrated Technology (IIT), Gwangju Institute of Science and Technology

ABSTRACT

While passive thermal imaging of temperature difference between tumor and neighboring tissue provides limited contrast, active thermography with external thermal modulation may provide higher contrast presumably due to the distinct thermal response from the tumor tissue. We have investigated physiologically relevant parameters such as response rate with respect to thermal modulation and relaxation time. This new imaging modality in the infrared regime may prove useful as a label-free and non-invasive screening tool. On the other hand, we propose a novel use of controlled thermal injury from non-ablative fractional laser irradiation for early treatment of tumor growth with a fiber-based thulium laser at 1927 nm. We investigated the potential cancer prevention effect with mouse model of early tumor. This laser treatment could potentially be an alternative anticancer modality for early tumorigenesis in a minimally invasive manner.

Tumor Detection by Means of Thermography

BACKGRODUN AND GOAL

- While thermography approach has a great advantage of no need of exogenous contrast agents and no ionizing radiation exposure for tumor detection, conventional passive thermography still lacks enough contrast to be used for early tumor detection.
- We propose active thermodynamic contrast imaging (ATCI) with external thermal modulators to provide more physiologically relevant parameters with high contrast such as the rate of temperature change, and thermal recovery time for tumor detection with a murine xenograft tumor model.

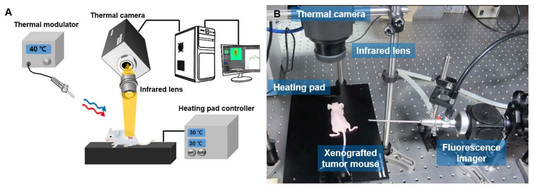

Experimental setup of active thermodynamic contrast imaging. (A) Schematic diagram of experimental setup. (B) Photograph of the setup consists of a thermal camera and a fluorescence imager. The thermal camera has a standard f 10 mm infrared imaging lens.

MATERIALS AND METHODS

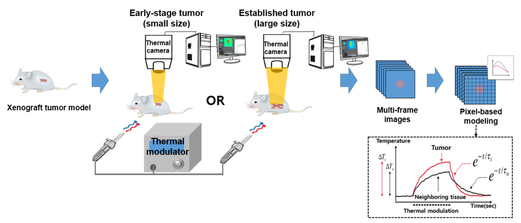

Active thermodynamic contrast imaging experimental procedure. After generation of a subcutaneous tumor (SL4-DsRed cancer cell) to the right flank, the thermal imaging of sequential temperature distribution throughout the convection modulation on the skin with subcutaneous tumors. With the same animal, the data collection was performed when the tumor was at an early-stage and in its established stage using the thermal camera. After data collection, the time series of images were processed with custom-written software. An exemplary data figure is depicted in the dotted lined box.

EXPERIMENTAL RESULTS

◆ Active thermodynamic imaging using convection modulation on early-stage tumors

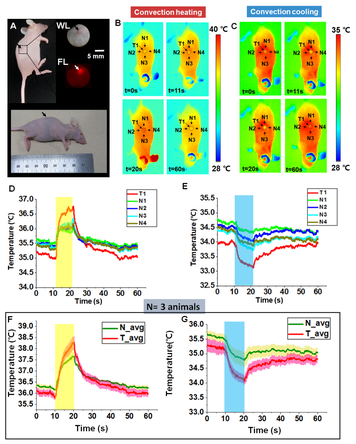

Thermal contrast imaging using convection thermal modulator with early-stage tumors. (A) Photograph of SL4-DsRed tumor-bearing mouse model. WL: white light image, FL: fluorescence image. (B, D) and (C, E) are representative sequential thermal images, and temperature changes over time in tumor and neighboring areas for heating and cooling, respectively from one animal. (F, G) shows the average and standard deviation in from all the animals in tumor and neighboring areas. The vertical shaded columns in F and G indicates the duration of thermal modulation for 10 secs for heating and cooling, respectively (n = 3 animals).

◆ Active thermodynamic imaging using convection modulation on established tumor

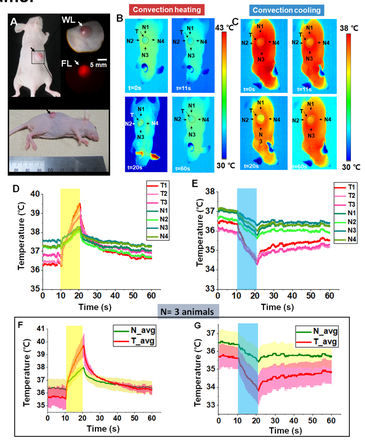

Thermal contrast imaging using convection thermal modulator with established tumors. (A) Photograph of SL4-DsRed tumor-bearing mouse model. WL: white light image, FL: fluorescence image. (B, D) and (C, E) are representative sequential thermal images, and temperature changes over time in tumor and neighboring areas for heating and cooling, respectively. (F, G) shows the average and standard deviation in from all the animals in tumor and neighboring areas. The vertical shaded columns in F and G indicates the duration of thermal modulation for 10 secs for heating and cooling, respectively (n = 3 animals).

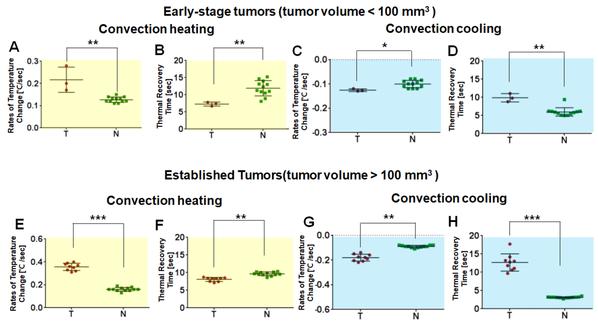

The rate of temperature change and the thermal recovery time (τ) between tumor and neighboring tissue for active thermal imaging at xenograft mice model (n = 3). (A-D) Early-stage tumor and its neighboring tissue. (E-H) Established tumor and its neighboring tissue. (A-B) The comparison graph between early-stage tumor and neighboring tissue using heating modulation. (A) The rate of temperature change values. (B) Thermal recovery time during the recovery period. (C-D) The comparison graph between tumor and neighboring tissue using cooling modulation. (C) The rate of temperature change. (D) Thermal recovery time during the recovery period. (E-F) The comparison graph between established tumor and neighboring tissue using heating modulation. (E) The rate of temperature change values. (F) Thermal recovery time during the recovery period. (G-H) The comparison graph between established tumor and neighboring tissue using cooling modulation. (G) The rate of temperature change. (H) Thermal recovery time during the recovery period, respectively (n = 3 animals). The error bars are standard deviations from all the ROI data (i.e. total 3 for early-stage tumors and 9 for established tumors while 12 for all the neighboring tissues). * P < 0.05, ** P < 0.01, *** P < 0.001 unpaired t-test)

CONCLUSION

- With early-stage tumors, we found the average rate of temperature change was higher in the tumor (0.22 ± 0.06 ℃/sec) than that of neighboring tissue (0.13 ± 0.01 ℃/sec) with heating modulation. With established tumors (volume > 100 mm3), this tendency was greater. On the other hand, the thermal recovery time was shorter in tumor tissue (τ = 7.30 ± 0.59 sec) than that of neighboring tissue (τ = 11.92 ± 2.22 sec).
- These results imply that there may exist different thermophysiological mechanisms involved when the tumor tissue recovers from heated or cooled states to its original conditions in comparison with its neighboring tissue. The underlying assumption for the calculation of recovery time constant is based on exponential model such as recovery time.

Tumor Treatment by Means of Laser Irradiation

BACKGRODUN AND GOAL

- Fractional laser resurfacing is a minimally invasive treatment that delivers small doses of laser light to biological tissue.
- We proposed that a stromal 'wounding' response to cosmetic NAFL therapies can prevent skin carcinogenesis or delay tumorigenesis. This proposed approach is related to the growing appreciation for the role of the tissue microenvironment

MATERIALS AND METHODS

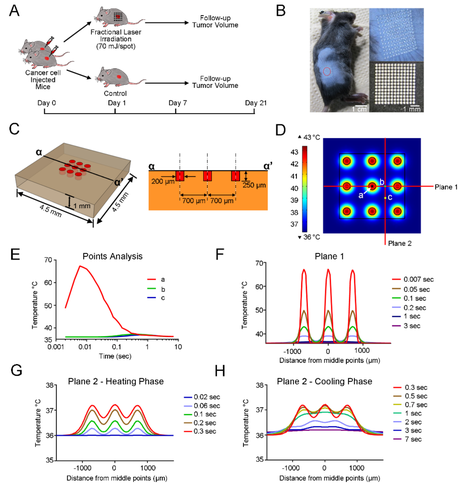

Non-ablative fractional laser (NAFL) irradiation of the xenograft tumor model. (A) Schematic illustration of the experiment. Cancer cell injected mice were divided into irradiation and control groups. NAFL (70 mJ/spot) was applied to the irradiation group, whereas no irradiation was delivered to the control group. The serial tumor volume was followed to measure the therapeutic efficacy of NAFL irradiation from day 7 to 21. (B) NAFL irradiated mouse. Left: NAFL irradiated SL4-DsRed tumor model mouse (red-dotted circle: cancer cell injected site). Right upper: Magnified image of flank lesion. Right lower: Array of NAFL irradiated spots on a black paper. (C) Schematic illustration of the tissue model for numerical simulation. Left: 3D image of the tissue model. Right: Cross-cut image of the 3D tissue model with plane α–α'. (D) Three representative spots and two image planes for temporal and spatial analysis. (E) Temporal distribution of the temperature changes at points a, b, and c. (F) Spatial distribution of the temperature in the tissue model along Plane 1. (G, H) Spatial distribution of the temperature during heating (G) and cooling (H) in the tissue model along plane 2.

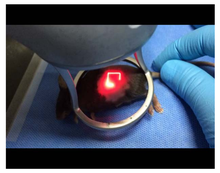

Non-ablative fractional laser (NAFL) irradiation to the skin area of the cancer cell-bearing mouse model. A 70 mJ/spot of energy was delivered to the mouse skin. Because the thulium laser wavelength is invisible to the naked eye, a 635 nm red diode laser was used to guide the irradiation

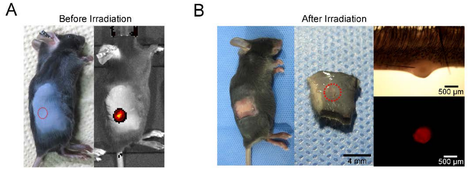

Optical imaging of SL4-DsRed tumor mouse before and after non-ablative fractional laser (NAFL) irradiation. (A) Fluorescence imaging of a SL4-DsRed cancer cell injected mouse using an optical imaging system (IVIS Luminar II, Caliper Life Sciences, Hopkinton, MA, USA). Excitation (535 nm) and emission (580 nm) filters were applied to find specific fluorescence signals from cancer cells. Left: photo image shows no significant elevated lesion 1 day after cancer cell injection (red-dotted circle: cancer cell injection site). Right: Fluorescence image from an optical imager (IVIS Luminar II). (B) Ex vivo confirmation of viable cancer cells after NAFL irradiation. Left: Excised flank skin from an SL4-DsRed injected mouse right after NAFL irradiation. Middle: Magnified image of the excised tissue. Right upper: White light image of the excised tissue slice. Right lower: Fluorescence image of the excised tissue slice. The fluorescence signal was detected by using an upright microscope (CX41, Olympus, Japan) with a fluorescence filter module (DMG 2, Olympus, Japan). A 40% intensity of a 525 nm LED was used as the excitation light source (Touch bright, Live Cell Instrument, Korea) and the exposure time was 90 milliseconds.

EXPERIMENTAL RESULTS

◆ Growth suppression of the tumor by NAFL irradiation

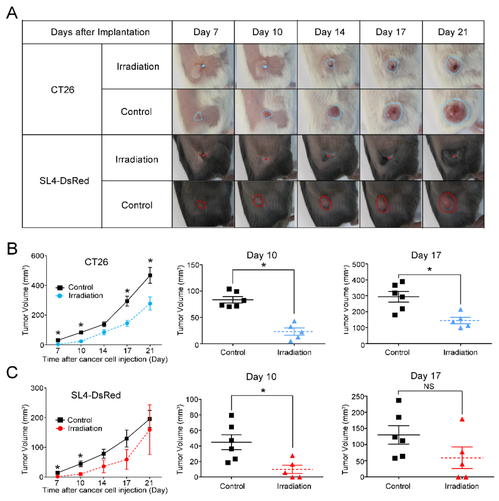

Tumor volume changes in xenograft tumor models. (A) Representative images of serial tumor volume (TV) changes during the follow-up periods. The blue- and red-dotted lines show the contour of the tumor. A single dot means no significant tumor lesion at the site. (B) In the CT26 implanted tumor model, the irradiation group (blue-dotted line) had smaller mean TVs (MTVs) than the control group (black solid line). On day 10 and day 17 after CT26 injection there is a statistically significant difference in MTVs between the irradiation and control groups. (C) In the SL4-DsRed tumor model, the irradiation group (red-dotted line) had smaller MTVs than the control group (black solid line). This difference in TV between the irradiation and control groups was observed on day 10 but not on day 17. Noticeably, 2 of the 5 SL4-DsRed cancer cell injected mice had shown no significant tumor growth until 90 days after cancer cell injection. Asterisk (*) indicates statistical significance < 0.05 while NS indicates no significance. All results are presented as mean ± SEM.

◆ An inflammatory reaction was induced by NAFL on day 1

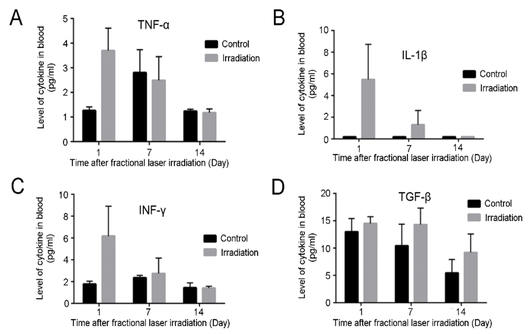

Cytokine analysis of SL4-DsRed tumor models. Enzyme-linked immunosorbent assays (ELISA) were performed to analyze the levels of the cytokines. (A) TNF-α, (B) IL-1β, (C) IFN-γ, and (D) TGF-β. TNF-α, IL-1β, and IFN-γ levels were elevated on day 1 after NAFL irradiation. TGF-β did not show any significance changes during the experimental period. All results are shown as mean ± SEM.

CONCLUSION

- We demonstrated the tumor growth suppression effect of NAFL with two syngeneic mouse models. To our knowledge, this is the first report on the use of NAFL as an anticancer stromal treatment modality.
- After controlled injury from NAFL irradiation, a local inflammatory change could regulate the early stage of tumorigenesis in a minimally invasive manner. Stromal NAFL irradiation has the potential to be an alternative, minimally invasive cancer therapeutic modality for early stages of tumorigenesis.

ACKNOWLEDGEMENT

We thank Mrs. Jihye Yang (from Department of Biomedical Science and Engineering, Gwangju Institute of Science and Technology) for preparation of SL4-DsRed cancer cell line and animal care and Mai Thi-Quynh Duong and Jin Hai Zheng (from Department of Nuclear Medicine, Chonnam National University Medical School and Hwasun Hospital, Jeonnam, Korea) for experimental help. This work was supported by Biomedical Integrated Technology Research Project, GIST Caltech Research Collaboration Project and the GIST Research Institute (GRI) provided by GIST in 2017, and by the Korean government (MEST) (No.NRF-2016R1A2B4015381)

REFERENCES

[1] SW Yoo, HJ Park, G. Oh, SJ Hwang, M. Yun, JJ Min, ES Kim, YL Kim, E. Chung, "Non-ablative fractional Thulium laser irradiation suppresses early tumor growth", Current Optics and Photonics, Vol. 1, Iss. 1, pp. 51-59 (2017)
[2] SW Yoo, G. Oh, A. M. Safi, SJ Hwang, M. Yun, ES Kim, YL Kim, E. Chung, "Non-ablative fractional thulium laser irradiation suppresses early tumor growth", submitted, 2017
[3] G. Oh, E. Chung, "Active thermodynamic contrast imaging for label-free tumor detection in a murine xenograft tumor model", submitted, 2017